Towards Optimal Automated 68 Ga-Radiolabeling Conditions of the DOTA-Bisphosphonate BPAMD Without Pre-Purification of the Generator Eluate

Céleste Souche, Juliette Fouillet, Léa Rubira, Charlotte Donzé, Audrey Sallé, Yann Dromard, Emmanuel Deshayes, Cyril Fersing

Journal of Labelled Compounds and Radiopharmaceuticals

WILEY

Journal of Labelled Compounds and Radiopharmaceuticals

RESEARCH ARTICLE OPEN ACCESS

Towards Optimal Automated ^{68}Ga-Radiolabeling Conditions of the DOTA-Bisphosphonate BPAMD Without Pre-Purification of the Generator Eluate

Céleste Souche[1] | Juliette Fouillet[1] | Léa Rubira[1] | Charlotte Donzé[1] | Audrey Sallé[1] | Yann Dromard[2] | Emmanuel Deshayes[1,2] | Cyril Fersing[1,3]

[1]Nuclear Medicine Department, Institut Régional du Cancer de Montpellier (ICM), Université de Montpellier, Montpellier, France | [2]Institut de Recherche en Cancérologie de Montpellier (IRCM), INSERM U1194, Institut Régional du Cancer de Montpellier (ICM), Université de Montpellier, Montpellier, France | [3]IBMM, Université de Montpellier, CNRS, ENSCM, Montpellier, France

Correspondence: Cyril Fersing (cyril.fersing@icm.unicancer.fr)

Received: 30 April 2024 | **Revised:** 1 October 2024 | **Accepted:** 1 November 2024

Funding: The authors received no specific funding for this work.

ABSTRACT

DOTA-functionalized bisphosphonates can be useful tools for PET imaging of bone metastases when radiolabeled with ^{68}Ga. Moreover, the versatility of DOTA allows the complexation of radiometals with therapeutic applications (e.g., ^{177}Lu), positioning these bisphosphonates as attractive theranostic agents. Among these molecules, BPAMD is a compound whose radiolabeling with ^{68}Ga has already been described, but only through manual methods. Thus, a fully automated protocol for ^{68}Ga radiolabeling of BPAMD on the GAIA® ± LUNA® synthesis module was designed, and a thorough study of the radiolabeling conditions was undertaken. [^{68}Ga]Ga-BPAMD was produced in good radiochemical purity (> 93%) and high radiochemical yield (> 91%) using 0.3 M HEPES buffer. The nature of the reaction vessel showed no significant effect on the radiolabeling outcome. Similarly, addition of an antiradiolysis compound to the reaction medium did not significantly improve the already excellent stability of [^{68}Ga]Ga-BPAMD over time. The radiolabeled product obtained by automated synthesis was evaluated in vivo in healthy mice and confirmed high accumulation in the joints and along the backbone.

1 | Introduction

Bisphosphonates (BPs) form an important therapeutic class used since the 1970s in the prevention and treatment of various bone diseases such as osteoporosis [1], fibrous dysplasia [2], Paget disease [3], hypercalcemia [4], or osteogenesis imperfecta [5]. Due to their high affinity for calcium ions in bone hydroxyapatite, BPs are also of great interest as delivery systems and targeting agents [6]. In particular, a number of BP-based vector molecules have been designed and studied for diagnostic applications such as MRI, fluorescence, single-photon emission computed tomography (SPECT), or positron emission tomography (PET) [7].

In clinical nuclear medicine, BPs are well-known for their formulation in lyophilized kits for ^{99m}Tc radiolabeling, used for bone scintigraphy [8]. The simplest BP derivative, medronate, was the first to be introduced as a radiopharmaceutical single vial cold kit for ^{99m}Tc radiolabeling [9] and is still used in some countries for scintigraphic detection of bone areas with abnormal osteogenesis (in both oncological and noncancer indications). Just like all the BP derivatives, medronate is based on the P-C-P chemical moiety that mimics inorganic pyrophosphate and confers resistance to enzymatic hydrolysis [10] (Figure 1). Currently, [^{99m}Tc]Tc-oxidronate is the most widely used BP for bone scan, the hydroxy group on the central sp^3 carbon potentially participating in ^{99m}Tc complexation and increasing

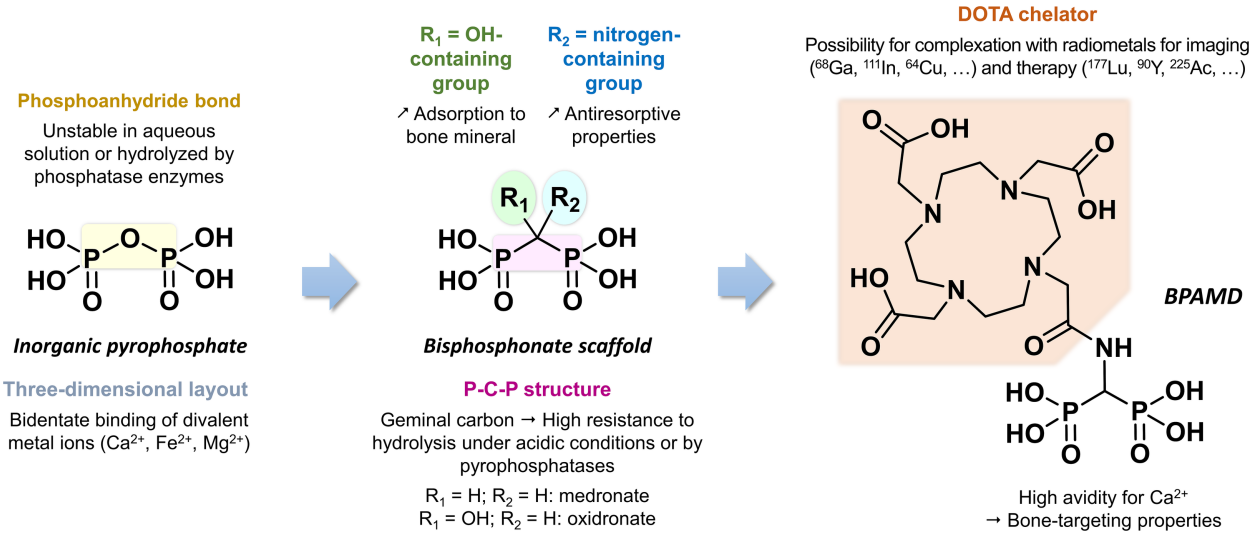

FIGURE 1 | Main structure-activity relationships in bisphosphonate series and chemical structure of BPAMD.

the radiopharmaceutical's affinity for bone mineral matrix. Besides, it is worth mentioning that other BP molecules bearing an additional nitrogen-containing group on the sp^3 carbon atom are rather used for their pharmacological properties and not as imaging agents [11, 12] (Figure 1). In the mid-2000s, BP derivatives functionalized with a DOTA chelator originally designed for Gd^{3+} complexation and MRI applications have been described [13–15]. Given the wide variety of metals that DOTA can complex, radiolabeling of such DOTA-BPs with gallium-68 ($t_{1/2}$ = 67.7 min, β^+ = 89%, electron capture = 11%) was rapidly considered, in view of their use as PET imaging agents [16–20]. The most straightforward of these compounds is BPAMD (bisphosphonate-amidomethyl analog of DOTA), used for the first time in human in 2010 for PET imaging of bone metastases from prostate cancer [21]. It was associated with very high target to soft tissues ratios and fast clearance and was later compared with [^{99m}Tc]Tc-medronate for the detection of bone metastases (mostly prostate cancer), allowing the detection of more lesions on PET scans [22].

In addition to the excellent resolution offered by PET imaging technology, the strength of DOTA-BPs lies in their suitability for theranostic approaches. In such perspective, therapeutic applications are brought closer to diagnostic purposes by complexing a particle-emitting radioelement instead of ^{68}Ga. This could be either a beta minus emitter such as ^{177}Lu [23–27] or an alpha emitter such as ^{225}Ac [28]. In that way, in-house preparation protocols of [^{177}Lu]Lu-BPAMD were developed for routine production to treat patients with skeletal metastases [29, 30]. Radiolabeling of BPAMD with yttrium-90 [31, 32], samarium-153 [33], holmium-166 [34, 35], and ytterbium-175 [36, 37] for targeted radionuclide therapy purposes was also reported.

For both diagnostic and therapy applications, automated radiolabeling of experimental radiopharmaceuticals not available in cold kit formulation is now a standard in clinic [38], in order to ensure good manufacturing process (GMP) specifications and meet national regulatory requirements [39]. Such preparation method is associated with increased radiolabeling yields, reliable and robust production processes, and reduced radiation exposure for operators [40]. Initial reports described manual synthesis of [^{68}Ga]Ga-BPAMD [17, 41]; however, no detailed automated ^{68}Ga radiolabeling protocol for BPAMD has yet been reported, and only a freeze-dried cold kit formulation was proposed [42]. In addition, automated preparation of other ^{68}Ga-labeled BP derivatives such as DOTAZOL was described as particularly challenging [43, 44]. More specifically, significant issues were identified concerning overall process automation, terminal purification, and quality controls reliability.

Hence, the purpose of the present work was to design a fully automated protocol for [^{68}Ga]Ga-BPAMD preparation on a GAIA®/LUNA® synthesis module and to study in-depth the radiolabeling conditions by varying several reaction parameters such as the buffer solution, the presence of an antiradiolysis compound, the amount of vector, the purification method, or the type of reaction vial. Reaction conditions that gave the highest radiochemical yields (RCY) and radiochemical purity (RCP) without prepurification of the generator eluate have therefore been identified. Finally, the radiocomplex obtained with optimal reaction conditions was tested in vivo using μPET/CT.

2 | Experimental

2.1 | Reagents, Solvents, and Apparatus

2.1.1 | General Considerations

Chemicals used for radiolabeling reactions were purchased from Merck (Darmstadt, Germany) and were of the highest available purity grade. Water for injection (WFI) and sodium chloride 0.9% were of pharmaceutical grade. Radiolabeling optimization assays were conducted on a GAIA® V2/LUNA® synthesis module (Elysia-Raytest, Germany) controlled by the appropriate software (GAIA control, Elysia-Raytest, Germany) and using disposable synthesis cassettes (Fluidic kit RT-01-H ABX, Advanced Biochemical Compounds, Germany). Between each automated radiolabeling, the cassette installed on the module was rinsed with WFI according to an automated sequence

configured for this purpose. The manifolds were then conserved for the next assay, and the tubing was changed. Of note, these non-GMP conditions are only suitable for automated radiochemistry assays; sterile cassettes must be single use if the GMP requirements have to be met. BPAMD (1,4,7,10-tetraazacyclododecane-1,4,7-triacetic acid, 10-[2-[(diphosphonomethyl)amino]-2-oxoethyl]) for radiolabeling assays was purchased from ABX (Germany). A stock solution of 1 mg/mL BPAMD in WFI was initially prepared and aliquoted into Eppendorf tubes (Protein LoBind Tubes 1.5 mL) to get 30 µg/30 µL fractions, stored at −20°C for up to 3 months. Gallium-68 was eluted from a pharmaceutical grade $^{68}Ge/^{68}Ga$ generator (GALLI AD® 1.85 GBq, Ire Elit, Belgium) and obtained under its $[^{68}Ga]GaCl_3$ form in 0.1 N HCl solution (1.1 mL per elution) that was not further purified. The [^{68}Ga]Ga-BPAMD production was conducted in a grade A shielded cell (MEDI 9000 Research 4R, LemerPax, La Chapelle-sur-Erdre, France) meeting GMP requirements, with the automated synthesis modules and the $^{68}Ge/^{68}Ga$ generator placed in the hot cell. Radioactivity in the product vial and residual radioactivity in the reaction vial, waste vial, purification cartridge, and terminal filter were measured in a calibrated ionization chamber (CRC®-25R, Capintec, USA) and corrected to the end time of radiolabeling to calculate RCY.

2.1.2 | Buffer Solutions Preparation

The buffers tested for [^{68}Ga]Ga-BPAMD automated preparation were chosen regarding their pKa value(s). The concentration used for each buffer was based on ^{68}Ga radiolabeling conditions reported in the literature. Each buffer solution was prepared extemporaneously before radiolabeling assays. The expected amount of buffer was measured on a calibrated precision balance with a single-use plastic spatula into a sterile single-use type 1 glass bottle and solubilized in WFI. For each buffer solution, the pH was adjusted with 37% HCl so that a predetermined 1.5 mL volume of buffer solution added to 1.1 mL of 0.1 N HCl (representing the volume of eluate provided by the GALLI AD® generator) reached a pH close to 3.4, suitable for ^{68}Ga radiolabeling reactions [45]. The five buffer solutions tested were sodium acetate 0.4 M pH 4.1 [46], ammonium acetate 0.1 M pH 4.2 [47, 48], ammonium acetate 2 M pH 4.2 [49], 4-(2-hydroxyethyl)-1-piperazineethanesulfonate (HEPES) 0.3 M pH 3.8 [50], and sodium formate 1.5 M pH 4.2 [51].

2.2 | Preparation for Radiolabeling of BPAMD With Gallium-68

Before starting the radiolabeling sequence, the synthesis module was equipped with a disposable cassette according to one of the following two configurations (Figure 2):

- Configuration A: The GAIA® module was used alone. It is equipped with 15 manifolds, a heating block that receives the reaction vial, and a peristaltic pump to transfer liquids during the synthesis. This configuration was adopted for most of the conditions tested.
- Configuration B: The LUNA® extension was associated to the GAIA® main module. It was used to evaluate the

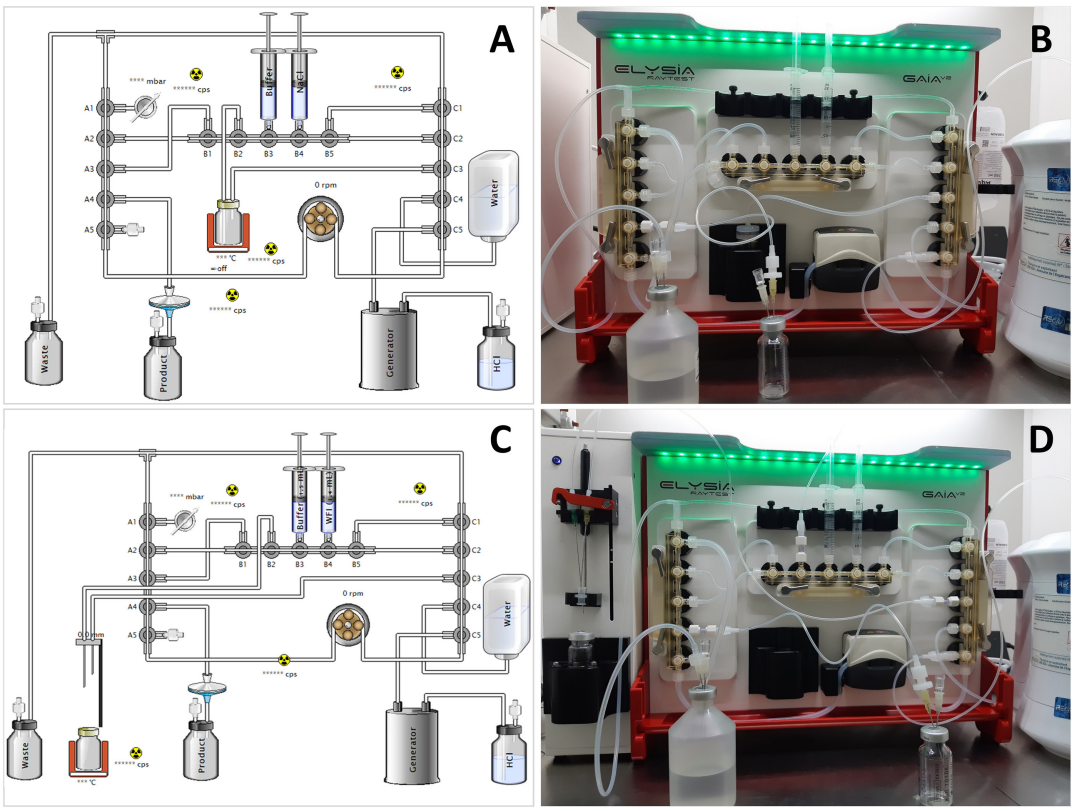

FIGURE 2 | Synthesis scheme (A, C) and cassette mounted in the module within the shielded cell (B, D) for the automated production of [^{68}Ga]Ga-BPAMD in configuration A (A, B) using a GAIA® module and configuration B (C, D) using GAIA® and LUNA® modules.

influence of the type of reaction vial on the radiolabeling reaction. This extension includes an additional heating block that can accommodate a variety of vials via a system of metal inserts. A hollow needle lift system allows to prick in the vial to transfer liquids during the automated synthesis.

If needed during assays, purification cartridges were properly preconditioned. Finally, the correct amount of BPAMD (30 to 50 μL of 1 mg/mL aliquots in WFI) was added to 1.5 mL of the desired buffer solution and connected to the cassette. Each modification of the reaction conditions was studied by performing the related automated assay in triplicate. Values of RCP and RCY obtained for each triplicate were expressed as mean ± standard deviation.

- To study the influence of the reaction buffer, BPAMD was dissolved in a predefined 1.5 mL volume of different buffer solutions with strictly controlled pH before starting the automated synthesis.
- To study the influence of the amount of vector, radiolabeling assays were performed by adding 30 or 50 μg of BPAMD in the buffer solution before starting the automated synthesis.
- To study the influence of the reaction vial model, as this was reported to be an important parameter for efficient radiolabeling of other DOTA-bisphosphonates [43], [^{68}Ga]Ga-BPAMD preparation was performed in automated configuration A with the GAIA® kit captive vial and in automated configuration B using either a 10 mL TechneVial® (Curium, France) or a 10 mL of FILL-EASE™ vial (Huayi Isotopes Co., China).
- To study the influence of the postradiolabeling purification step of [^{68}Ga]Ga-BPAMD, the cassette installed on the synthesis module was equipped with a ready-to-use strong cation exchange (SCX) cartridge (Chromabond® PS-H$^+$ size M, Macherey-Nagel, Germany), a custom SCX cartridge (Strata-X-C 33 μm 10 mg/1 mL, Phenomenex, USA) connected to the synthesizer using a luer adapter cap (Bond Elut adapter for 1, 3 and 6 mL, Agilent, USA), or no purification cartridge. SCX cartridges were preconditioned by washing successively with 5 mL of 0.1 N HCl and 5 mL of WFI.
- To study the influence of an antiradiolysis compound on the RCP over time, the buffer solution was added with 0.1 mL of freshly prepared ascorbic acid 10 mg/mL, gentisic acid 16 mg/mL, or methionine 10 mg/mL solution. The stability of the final product [^{68}Ga]Ga-BPAMD at room temperature was then monitored, measuring RCP by radio-high-performance liquid chromatography (radio-HPLC) at 0.5, 1, 2, 3, and 4 h after the radiosynthesis.

2.3 | Automated Radiolabeling Process of BPAMD With [^{68}Ga]GaCl$_3$

After initialization of the synthesis sequence, the module performed a kit integrity test to prevent any leakage during preparation. Then, if installed, the solid phase extraction (SPE) cartridge connected between A2 and B1 valves was conditioned with WFI before the tubing lines were purged with filtered air. BPAMD contained in 1.5 mL of buffer solution was transferred to the reaction vial, and the ^{68}Ge/^{68}Ga generator was eluted with 1.1 mL of 0.1 N HCl, the unprocessed elution being transferred to the reaction vial preheated at 60°C. The radiolabeling reaction proceeded for 12 min at 97°C. The reaction medium was then transferred in the product vial with no further purification or after passing through a SCX cartridge. The reaction vial was rinsed with 2.4 mL of WFI that were also transferred subsequently in the product vial (total theoretical volume of final product = 5 mL). Terminal sterilizing filtration was provided by a 0.22 μ end filter (Millex®-GV 0.22 μ 1.3 cm, Merk, NJ, USA); integrity of the filter was checked by the module at the end of the preparation by a bubble point integrity test [52]. The overall automated process of [^{68}Ga]Ga-BPAMD radiosynthesis is summarized in Figure 3, and the detailed automated sequences are provided in the Supporting Information.

2.4 | Quality Controls

2.4.1 | TLC RCP Assessment

Radio-thin layer chromatography (TLC) analyses were performed in accordance with a protocol inspired by the literature [20], using a TLC silica gel F254 plate coated on aluminum foil (2 cm × 9 cm). A small drop of [^{68}Ga]Ga-BPAMD was placed on the plate 1 cm above the base line. The plate was then placed in a development chamber containing an acetylacetone/acetone mixture (1:1) supplemented with 5% (v/v) of 37% HCl. The mobile phase was allowed to migrate approximately 0.5 cm below the top end of the strip. It was then removed from the chamber and placed into a TLC scanner (miniGITA® Star, Elysia-Raytest, Germany) to determine the % areas of radioactivity at the origin and at the solvent front, using the appropriate acquisition software (TLC Control v.2.30, Raytest, Germany) and analysis software (GINA Star TLC™ v.6.0, Elysia-Raytest, Germany). Under these conditions, R_f ([^{68}Ga]Ga-BPAMD) = 0.0–0.2 and R_f (^{68}Ga colloids + $^{68}Ga^{3+}$) = 0.8–1.0. Radio-TLC spectra of method validation assays are provided in the Supporting Information.

2.4.2 | HPLC RCP Assessment

Radio-HPLC analyses were carried out on a Nexera X3 apparatus (Shimadzu, Japan) using HPLC-grade solvents, in accordance with a protocol inspired by literature [53]. UV detection was set at 220 nm, and radioactivity detection, using a GABI Nova detector (Elysia-Raytest, Germany), was set at 400-600 keV window. The stationary phase was a C_{18} ACE® Equivalence™ column, 3.0 × 150 mm, 110 Å pore size, and 3 μm particles size. The flow rate was 0.3 mL/min, and the mobile phase was di-sodium hydrogen phosphate dihydrate 0.08 mM with N,N-dimethylhexylamine 0.03 M and ortho-phosphoric acid 0.18 M (pH 3) in isocratic mode. Radio-HPLC analyses were performed using the appropriate acquisition and analysis software (Gina Star 10, Elysia-Raytest, Germany). Radio-HPLC spectra of method validation assays are provided in the Supporting Information.

2.4.3 | pH Measurements

During buffer solutions preparation, pH was initially checked using both 2-zones Rota pH 1–11 indicator paper (VWR, PA,

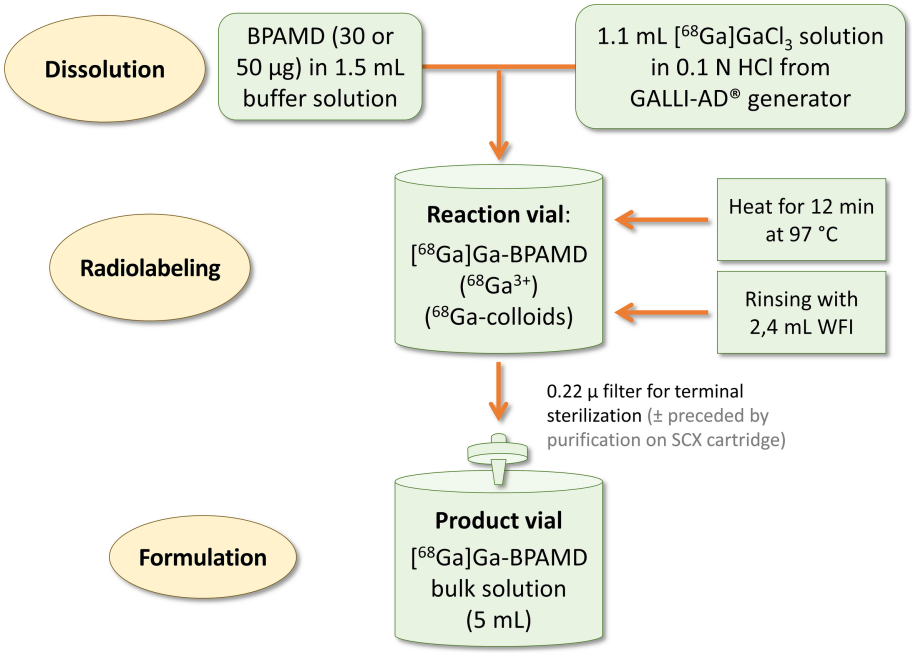

FIGURE 3 | Flow chart for [^{68}Ga]Ga-BPAMD synthesis process.

USA) and MQuant® pH 2.5–4.5 indicator strips (Merk, NJ, USA). Then, pH value was confirmed using a recently calibrated Vario® pH meter (WTW®, Xylem, USA) equipped with a SenTix® 41 pH electrode (WTW®, Xylem, USA). The pH of the HPLC mobile phase and of the final product [^{68}Ga]Ga-BPAMD was checked using only 2-zones Rota paper.

2.5 | Animal Studies

PET imaging was performed in spontaneously breathing athymic nude mice under isoflurane anesthesia (2% isoflurane, 98% filtered air). [^{68}Ga]Ga-BPAMD was prepared following the described protocol with 30 µg of ligand. Syringes for injection were measured in a calibrated ionization chamber (CRC®-55 t, Capintec, USA). Each mouse ($n = 3$) was injected intravenously (tail vein infusion, ~0.5 mL/min) with 18.9 ± 0.6 MBq of [^{68}Ga]Ga-BPAMD (V ~ 0.4 mL) at 30-, 45-, and 60-min postsynthesis (specific activity injected ~17, 15 and 12.5 MBq/µg, respectively; RCP of the preparation = 92.71% determined by HPLC). The µ-PET imaging was performed on a microPET nanoScan®PET (Mediso, Hungary). During PET measurements, animals were placed in prone position, with their medial axis parallel to the axial axis of the scanner. PET acquisitions were performed 1-h postinjection, lasted 15 min, and were followed by whole body CT-scan acquisition (Nucline™ software, RS^{2}D, France). Finally, PET acquisitions were reconstructed in static 3D mode (Nucline Tera-Tomo™ software, RS^{2}D, France).

2.6 | Statistical Analysis

Two-sided Wilcoxon rank sum test was used to compare triplicate RCP or RCY values obtained under two different reaction conditions. The p-value was used to estimate statistical significance ($p < 0.05$ considered as significant).

3 | Results and Discussion

Two fully automated protocols for [^{68}Ga]Ga-BPAMD synthesis were developed. The first sequence involved the GAIA® module only (configuration A, Figure 2A,B) and lasted 22 min from the start of the synthesis to the delivery of the radiolabeled compound in the product vial. The second sequence was based on the combined GAIA®/LUNA® modules (configuration B, Figure 2C,D), lasted 23.5 min and allowed the use of different reaction vial models. In order to define a radiolabeling protocol that is as straightforward as possible and to facilitate its automation, it was decided to use the gallium eluate directly without prepurification, thus shortening the synthesis time.

The influence of several parameters involved in the radiolabeling reaction of BPAMD with ^{68}Ga was then directly studied at the scale of the automated reaction, as the strict transposition of best manual radiolabeling conditions frequently requires reoptimization [54, 55]. To this end, we compared RCP and RCY values (measured by both TLC and HPLC) for each condition studied. Importantly, the mean residual activity on the terminal filter (0.94 ± 0.78 MBq over the 33 assays) was assumed negligible and was not considered in the RCY calculations. The effective final volume was checked by gravimetry on three test syntheses (assuming that the density of the liquids composing the final mixture is 1 g/mL) and was 4.97 ± 0.05 mL, that is, a deviation of −0.6% from the theoretical value of 5 mL.

The study of the ^{68}Ga radiolabeling conditions of BPAMD was initiated by investigating the influence of the reaction buffer. Widely described in other automated ^{68}Ga radiolabeling protocols [56–63], sodium acetate at 0.4 M concentration was first used, leading to modest RCP and RCY values (around 53% and 52%, respectively). Moreover, the results obtained in the three assays carried out with these conditions were

poorly repeatable (Figure 4). Reported in the literature in manual [^{68}Ga]Ga-BPAMD preparation protocols [17], ammonium acetate at high concentration (2 M) was then evaluated in automated conditions and showed extremely poor results in terms of mean RCP (around 30%) and RCY (around 25%), still with considerable variability in results. Additionally, average residual activity in the reaction vial was higher with ammonium acetate 2 M than with the other buffers tested (10.2% of total radioactivity vs. 0.9% to 2.3 % of total radioactivity). This demonstrates that optimized manual radiolabeling conditions are rarely strictly transposable to an automated sequence [55]. The use of sodium formate 0.5 M produced comparable results. Interestingly, ammonium acetate at a tenfold lower concentration (0.2 M) allowed a very significant improvement in the mean RCP (from 30% to 90% RCP measured by HPLC) and RCY (from 25% to 86% RCY measured by HPLC) despite a persistent lack of reproducibility, particularly for RCP values obtained by radio-TLC. An explicit rationale for these unsatisfactory and unreproducible results is difficult to identify. This could partly be due to the chelating properties of certain buffers, including ammonium and sodium acetate, combined with the fact that the phosphonate groups of BPAMD could interact with $^{68}Ga^{3+}$ ions during radiolabeling. However, such assumptions are hardly verifiable. Finally, having already proved its undeniable interest in ^{68}Ga radiolabeling automated protocols [64–69], HEPES 0.3 M allowed excellent and minimally variable RCP and RCY to be achieved, according to both radio-TLC (93.1% and 92.0%, respectively) and radio-HPLC (95.9% and 94.7%, respectively) analyses.

The major drawback of the HEPES buffer remains, in several countries, its regulatory restriction within radiopharmaceuticals for human use. Indeed, even though the concentrations used in our study are low (~107 mg in 5 mL final volume), the European Pharmacopeia set, for example, a regulatory limit for HEPES at <500 µg per injected dose of radiopharmaceutical (i.e., around 200 times less than herein) [70, 71]. This buffer having no monograph in the Ph. Eur., it is considered as a chemical impurity. Nevertheless, the literature still mentions the use of HEPES for ^{68}Ga radiolabeling of BPAMD, like in the kit-based formulation proposed by Guleria et al. that contains HEPES in slightly higher quantities than in the present study (~150 mg per preparation versus ~107 mg in our case) [42]. The same applies to the semi-automated method for [^{68}Ga]Ga-BPAMD preparation described by Vatsa *et al*. which uses 150 mg HEPES per reaction [22]. Thus, although considered suitable for human use [72], a terminal purification step is usually required to remove HEPES buffer from the final product, which is a particularly difficult operation to implement for small hydrophilic molecules such as [^{68}Ga]Ga-bisphosphonates [43]. Moreover, HEPES residue must also be evaluated during the quality controls of the radiopharmaceutical preparation [73–76]. Although in vivo tolerance studies of HEPES have been carried out [77–79], the lack of toxicological data is generally cited as the main reason for the regulatory

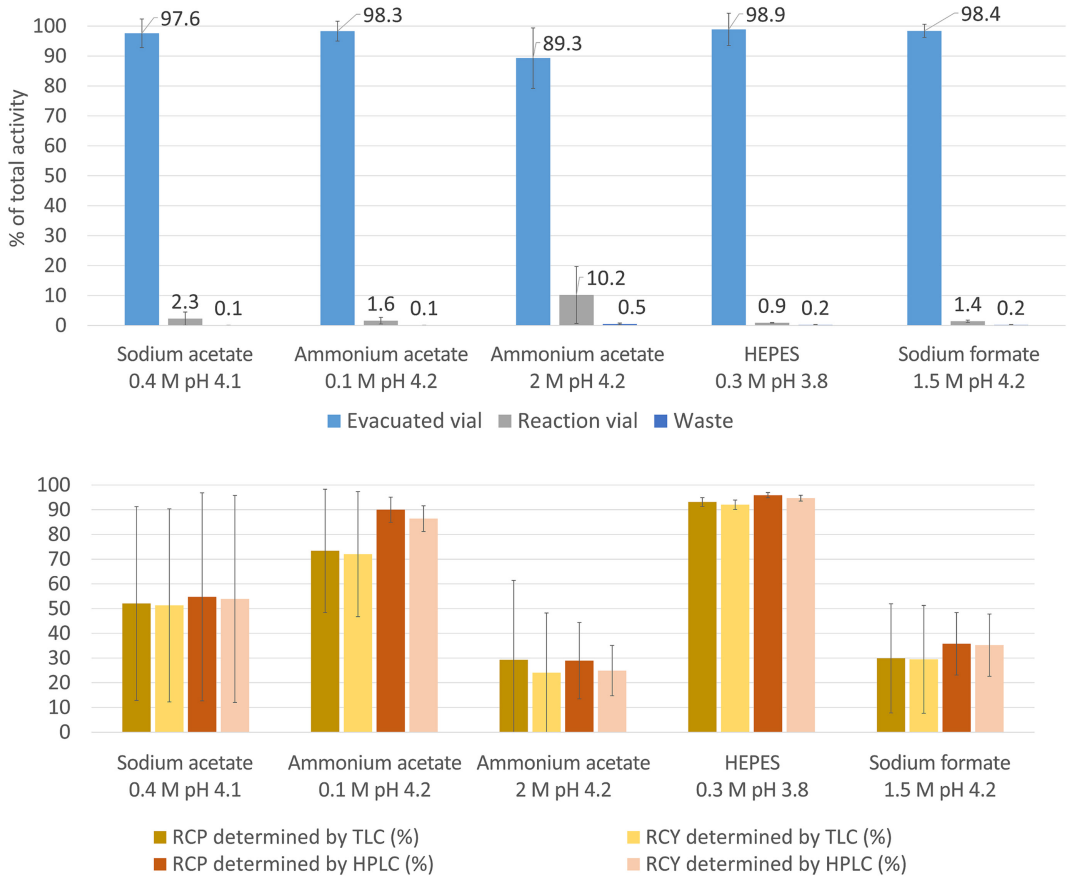

FIGURE 4 | Activity distribution in the cassette (up) and RCP and RCY values measured by TLC and HPLC (down) depending on the reaction buffer.

limits of this buffer in radiopharmaceuticals [45]. Consequently, further toxicological studies in animals or humans, combined with the intention of regulatory authorities to facilitate the use of HEPES buffer, could ideally lead to its wider use in radiopharmaceutical preparations in the future [80]. Overall, in view of the excellent results obtained with this buffer, HEPES 0.3 M was retained for all subsequent assays.

The radio-TLC conditions used for RCP determination of [^{68}Ga]Ga-BPAMD were directly taken from literature [20]. In the acetone/acetylacetone/hydrochloric acid (1/1/0.1) mobile phase, gallium colloids are expected to be converted into free gallium, all uncomplexed [^{68}Ga]Ga^{3+} ions subsequently forming a chelate with acetylacetone which migrates with the solvent front (Figure 5). Although a lack of reliability of this method has been reported for other ^{68}Ga-bisphosphonates [43], no false negative analysis has apparently been reported in the literature for quality controls of [^{68}Ga]Ga-BPAMD [17, 41]. Moreover, throughout the present study, no significant discrepancies were identified between RCP values determined by radio-TLC and corresponding PRC values determined by radio-HPLC. The weakness of this radio-TLC protocol, however, is its failure to discriminate between free gallium and gallium colloids impurities. The radio-HPLC conditions were inspired by the analysis method of a tetraphosphonate derivative, [^{68}Ga]Ga-EDTMP [53]. With this method, a conventional reversed-phase column is allowed to discriminate small, highly polar substances, thus avoiding the use of an anion exchange stationary phase. Conversely, particular attention must be given to the pH control of the mobile phase, as well as to the equilibration time of the system, which must be long enough to prevent variations in retention times (Figure 5).

Higher amount of BPAMD involved in the radiolabeling reaction was investigated in an attempt to increase the proportion of complexed [^{68}Ga]Ga^{3+}, and therefore improve RCP (Figure 6). Whether using 30 µg or 50 µg BPAMD, the RCP values obtained under either condition showed no significant difference, as measured by TLC ($p = 0.4$) or HPLC ($p = 0.4$). The same applied to RCY values, measured either by TLC ($p = 0.4$) or HPLC ($p = 0.7$). Similarly to other radiopharmaceuticals such as PSMA-11 or DOTATOC [81], previously reported single vial cold kit formulations of BPAMD involved the highest amount of vector molecule (50 µg) [22, 42], whereas manual preparation protocols used lower quantities of BPAMD (between 12 and 30 µg for optimal radiolabeling) [17, 41]. Therefore, in accordance with the literature, the amount of vector molecule was not increased in our

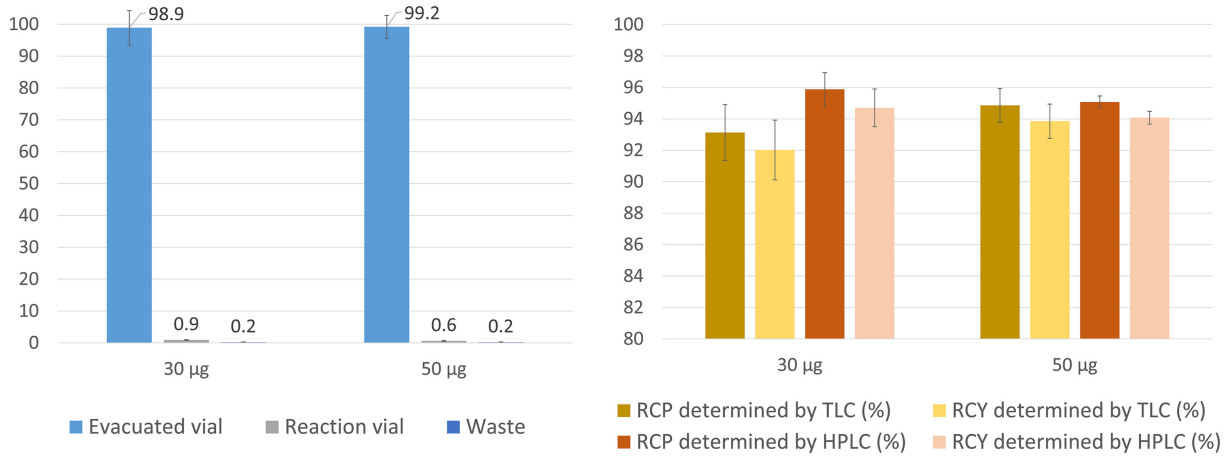

FIGURE 6 | Activity distribution in the cassette (left) and RCP and RCY values measured by TLC and HPLC (right) depending on the amount of BPAMD used for the radiolabeling reaction.

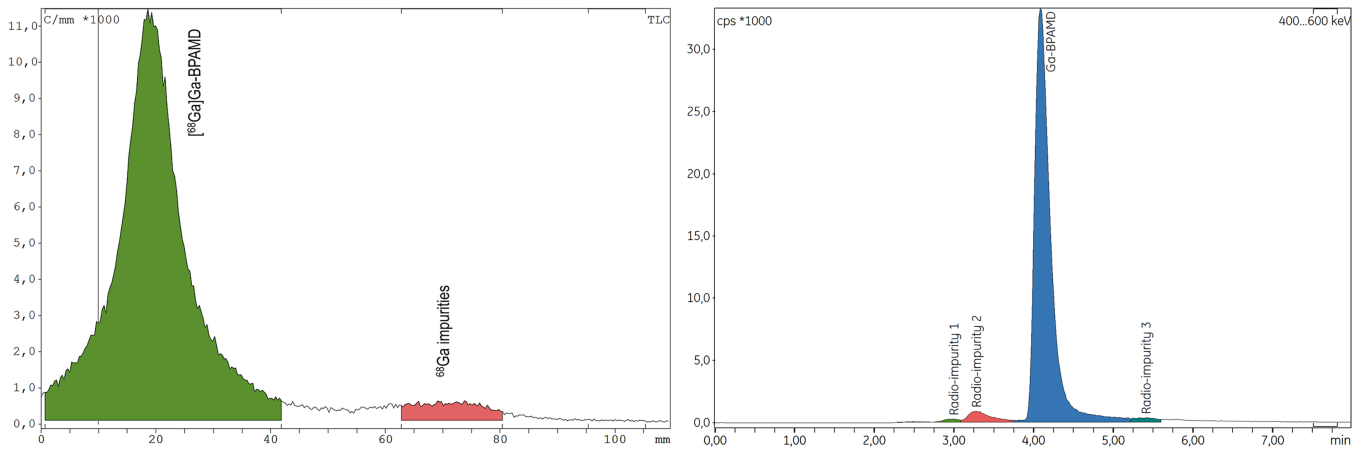

FIGURE 5 | Radio-TLC (left) and radio-HPLC (right) spectra of [^{68}Ga]Ga-BPAMD after radiolabeling with HEPES 0.3 M.

automated radiolabeling protocol and 30 μg BPAMD were used for the subsequent assays.

The influence of the reaction vial model on the overall outcome of the radiolabeling process was previously described as highly significant for another DOTA-conjugated bisphosphonate, DOTA-zoledronate [43]. We therefore studied this parameter during the automated preparation of [^{68}Ga]Ga-BPAMD by comparing the captive vial of the GAIA® module tubing set (configuration A) with two other vials commonly used for radiopharmaceuticals preparation, set up via the LUNA® module (configuration B). As shown in Figure 7, the use of a TechneVial® vessel did not result in significantly different performances from the captive vial, either for RCP measured by TLC ($p = 0.4$) and HPLC ($p = 0.4$) or for RCY measured by TLC ($p = 1$) or HPLC ($p = 0.4$). The same applied to the FILL-EASE™ vial, both for RCP measured by TLC ($p = 1$) and HPLC ($p = 0.1$) and for RCY measured by TLC ($p = 1$) and HPLC ($p = 0.1$). Notably, each of the three reaction vials contained very low residual activity at the end of synthesis (from 0.9% to 2.3% of total activity). Therefore, the proportion of radioligand adsorbed on the glass surface seems to rather depend on the bisphosphonate molecule [82]. Although not particularly beneficial for [^{68}Ga]Ga-BPAMD preparation, configuration B could therefore be used for radiolabeling of other vector molecules at risk of interaction with the glass vessel that would require special vials (e.g., with silicon dioxide or hydrophobic coating) [83].

Because of its low molecular weight and hydrophilic properties, BPAMD is not retained by conventional reverse-phase SPE cartridges. Protocols for the manual preparation of [^{68}Ga]Ga-BPAMD described purification with SCX column (Strata-X-C, Phenomenex) to retain free ^{68}Ga or with weak anion exchange column (Isolute NH2, Biotage) subsequently eluted with PBS [84]. The first assay undertaken in our study involved a sulfonylated polystyrene-divinylbenzene copolymer-based cartridge and led to extremely inconsistent results, with either partial purification of the ^{68}Ga complex or retention of a portion of the radiolabelled product (with TLC analyses: mean RCP = 66.1% ± 44.6% and mean RCY = 30.6% ± 29.9%; with HPLC analyses, mean RCP = 74.4% ± 35.6% and mean RCY = 31.6% ± 29.9%). The second assay with custom SCX cartridges connected to the synthesis module by a luer adapter only retained a small fraction of impurities (9.3 ± 3.1 MBq) and were associated with lower RCP (89.0% ± 5.3% determined by TLC and 87.8% ± 2.3% determined by HPLC). In addition, purification on SPE cartridge of other DOTA-bisphosphonates has proved extremely difficult to implement [43]; thus, this step has not been further explored at present. The good RCP achieved so far could dispense with terminal purification, especially as the use of a SCX cartridge would not remove HEPES buffer. Nevertheless, it is important to note that without a final purification step, particular attention should be paid to the possibility of ^{68}Ge breakthrough. Notably, purification of [^{68}Ga]Ga-BPAMD by preparative HPLC could effectively achieve RCP values > 95%. However, this method would require equipment that is not widely available in nuclear medicine departments.

The stability of ^{68}Ga radiopharmaceutical preparations is usually measured over 4 h [55]. In the present study, mean RCP of [^{68}Ga]Ga-BPAMD radiolabeled in HEPES buffer alone showed no decrease over this period (95.9% ± 1.1% right after radiolabeling to 93.8% ± 1.5% at 4-h postradiolabeling, Figure 8). Nonetheless, the influence of antiradiolysis compounds on the overall reaction course was studied, as the automated ^{68}Ga radiolabeling process of several innovative PET imaging agents involves such compounds (e.g., ascorbic acid [46, 85–87] or gentisic acid [56, 58, 59, 61]). Interestingly, the adjunction of gentisic acid 1.06 mg/mL to the reaction medium was associated with a notable decrease in RCP measured by HPLC at 30-min postsynthesis (from 90.8% ± 2.2% to 86.3% ± 0.7%), then remaining stable for up to 4 h. The RCP of [^{68}Ga]Ga-BPAMD over time after radiolabeling in the presence of ascorbic acid 0.67 mg/mL was very constant over 4 h (from 94.5% ± 0.3% to 93.7% ± 1.7%) and provided no evident benefit compared to HEPES only other than smaller variations in RCP between experiments. Consequently, ascorbic acid addition in the reaction medium was retained.

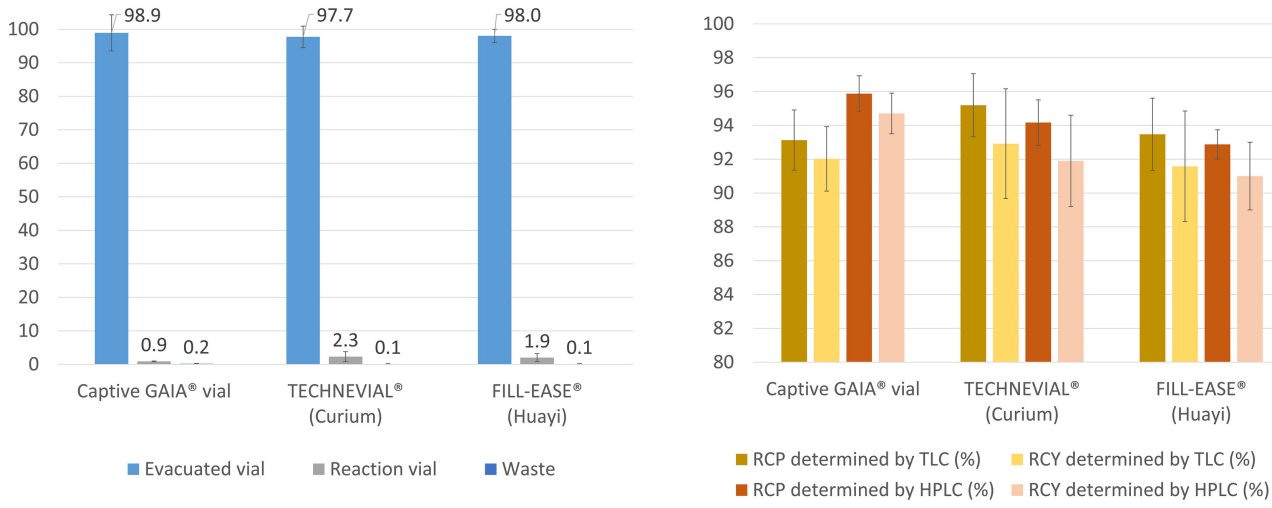

FIGURE 7 | Activity distribution in the cassette (left) and RCP and RCY values measured by TLC and HPLC (right) depending on the type of reaction vial.

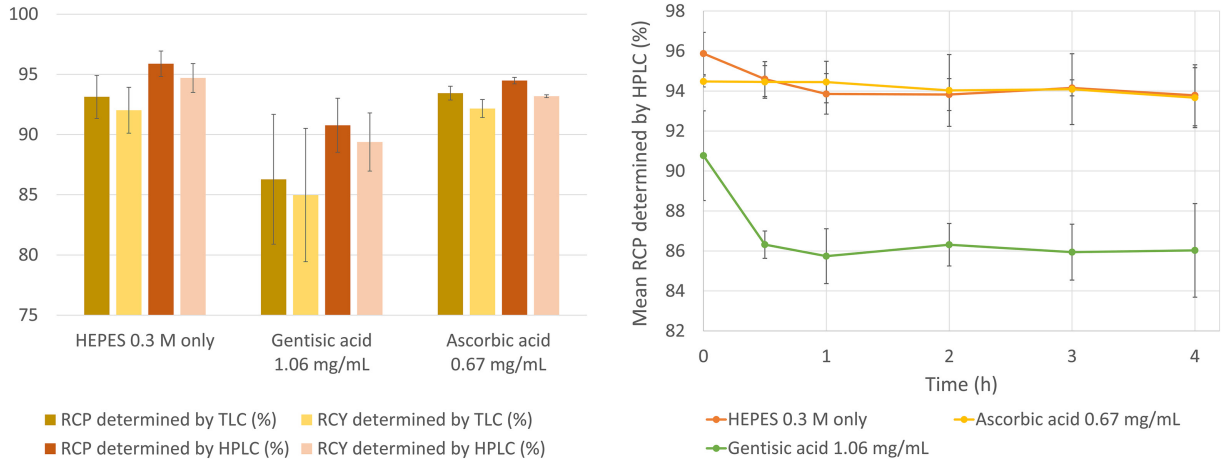

FIGURE 8 | RCP and RCY values measured by TLC and HPLC right after the synthesis (left) and time course of [^{68}Ga]Ga-BPAMD RCP measured by HPLC, with or without antiradiolysis compounds.

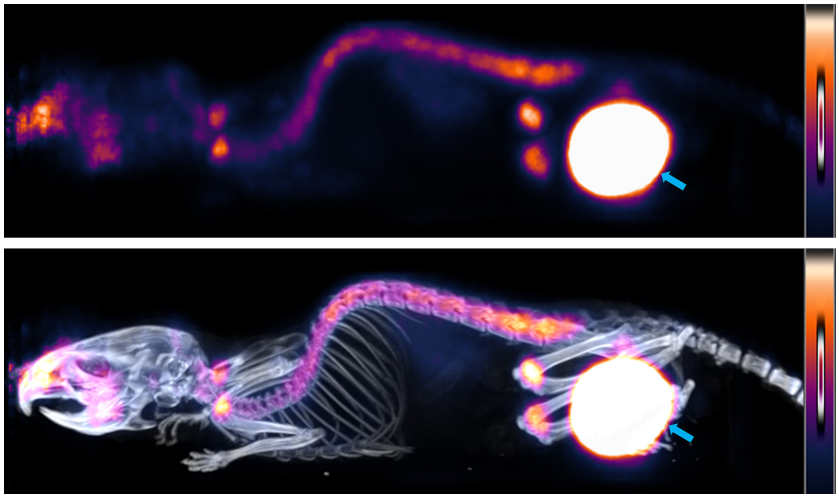

FIGURE 9 | Example of in vivo accumulation of [^{68}Ga]Ga-BPAMD (18.2 MBq) in bones of healthy mouse, IV tail vein injection, μPET (up) and μPET/CT (down) scans (MIP), 60 min p.i. Blue arrow shows intravesical retention due to urinary excretion.

Finally, [^{68}Ga]Ga-BPAMD synthesized using the optimized radiolabeling conditions previously discussed (HEPES 0.3 M, 30 μg vector molecule, captive vial of the GAIA® module, ascorbic acid 0.67 mg/mL) was injected to healthy mice for μPET imaging that confirmed expected high bone and joints uptake. Based on lumbar vertebrae uptake, the bone to soft-tissue ratio (taking liver as the reference soft tissue) was high (5.1 ± 1.5) 60-min postinjection in three mice. Figure 9 illustrates a significant uptake in the skeletal system of a mouse 60-min postinjection. The residual urinary activity observed within the bladder (blue arrow) corresponds to the expected urinary excretion of the radiotracer. Considering the RCP of the preparation used for these experiments, it is reasonable to postulate that traces of free gallium-68 may cause some gastrointestinal and vascular background as well as some nonspecific bone binding. Possible gallium-68 colloids may be responsible for hepatic or splenic background. Regarding other radioimpurities, it can be assumed that radiolabeled by-products still carrying the bisphosphonate motif would bind to bone in the same way as [^{68}Ga]Ga-BPAMD, while any radiolabeled by-products no longer expressing their vector moiety would most likely be eliminated directly via the kidneys. However, confirmation of these hypotheses would require characterization of the radioimpurities in question.

4 | Conclusions

An optimized method for automated production of [^{68}Ga]Ga-BPAMD on a GAIA® synthesis module was developed through an in-depth study of several radiolabeling reaction parameters. According to convenient radio-TLC and radio-HPLC methods, [^{68}Ga]Ga-BPAMD was obtained with > 93% RCP and > 91% RCY, in less than 25 min. The cassette-based automated process being GMP-compliant, it would facilitate upcoming clinical use of this PET imaging agent. At this point, the preclinical value of [^{68}Ga]Ga-BPAMD prepared that way has been demonstrated, and further studies need to be performed

to identify and implement an efficient, reliable terminal purification step, particularly to remove HEPES from the final product.

Acknowledgments

The authors thank Fiona Garnier for her help in the completion of this work.

Conflicts of Interest

The authors declare no conflicts of interest.

Data Availability Statement

The data used to support the findings of this study are included within the article or included within the supporting information file.

References

1. M. J. Favus, "Bisphosphonates for Osteoporosis," *New England Journal of Medicine* 363, no. 21 (2010): 2027–2035, https://doi.org/10.1056/NEJMct1004903.

2. M. Rotman, N. A. T. Hamdy, and N. M. Appelman-Dijkstra, "Clinical and Translational Pharmacological Aspects of the Management of Fibrous Dysplasia of Bone," *British Journal of Clinical Pharmacology* 85, no. 6 (2019): 1169–1179, https://doi.org/10.1111/bcp.13820.

3. L. Corral-Gudino, A. J. Tan, J. Del Pino-Montes, and S. H. Ralston, "Bisphosphonates for Paget's Disease of Bone in Adults," *Cochrane Database of Systematic Reviews* 12, no. 12 (2017): CD004956, https://doi.org/10.1002/14651858.CD004956.pub3.

4. S. Minisola, J. Pepe, S. Piemonte, and C. Cipriani, "The Diagnosis and Management of Hypercalcaemia," *BMJ* 350 (2015): h2723, https://doi.org/10.1136/bmj.h2723.

5. K. Dwan, C. A. Phillipi, R. D. Steiner, and D. Basel, "Bisphosphonate Therapy for Osteogenesis Imperfecta," *Cochrane Database of Systematic Reviews* 10, no. 10 (2016): CD005088, https://doi.org/10.1002/14651858.CD005088.pub4.

6. S. Sun, J. Tao, P. P. Sedghizadeh, et al., "Bisphosphonates for Delivering Drugs to Bone," *British Journal of Pharmacology* 178, no. 9 (2021): 2008–2025, https://doi.org/10.1111/bph.15251.

7. A. Kuźnik, A. Październiok-Holewa, P. Jewula, and N. Kuźnik, "Bisphosphonates—Much More Than Only Drugs for Bone Diseases," *European Journal of Pharmacology* 866 (2020): 172773, https://doi.org/10.1016/j.ejphar.2019.172773.

8. J. H. Thrall, "Technetium-99m Labeled Agents for Skeletal Imaging," *CRC Critical Reviews in Clinical Radiology and Nuclear Medicine* 8, no. 1 (1976): 1–31.

9. G. Subramanian, J. G. McAfee, R. J. Blair, F. A. Kallfelz, and F. D. Thomas, "Technetium-99m-Methylene Diphosphonate--A Superior Agent for Skeletal Imaging: Comparison With Other Technetium Complexes," *Journal of Nuclear Medicine* 16, no. 8 (1975): 744–755.

10. M. D. Francis, R. Graham, G. Russell, and H. Fleisch, "Diphosphonates Inhibit Formation of Calcium Phosphate Crystals in Vitro and Pathological Calcification in Vivo," *Science* 165, no. 3899 (1969): 1264–1266, https://doi.org/10.1126/science.165.3899.1264.

11. F. H. Ebetino, A. V. Bayless, J. Amburgey, K. J. Ibbotson, S. Dansereau, and A. Ebrahimpour, "Elucidation of a Pharmacophore for the Bisphosphonate Mechanism of Bone Antiresorptive Activity," *Phosphorus, Sulfur and Silicon and the Related Elements* 109, no. 1-4 (1996): 217–220, https://doi.org/10.1080/10426509608545129.

12. M. J. Rogers, J. Mönkkönen, and M. A. Munoz, "Molecular Mechanisms of Action of Bisphosphonates and New Insights Into Their Effects Outside the Skeleton," *Bone* 139 (2020): 115493, https://doi.org/10.1016/j.bone.2020.115493.

13. V. Kubícek, J. Rudovský, J. Kotek, et al., "A Bisphosphonate Monoamide Analogue of DOTA: A Potential Agent for Bone Targeting," *Journal of the American Chemical Society* 127, no. 47 (2005): 16477–16485, https://doi.org/10.1021/ja054905u.

14. T. Vitha, V. Kubícek, P. Hermann, et al., "Lanthanide (III) Complexes of bis (Phosphonate) Monoamide Analogues of DOTA: Bone-Seeking Agents for Imaging and Therapy," *Journal of Medicinal Chemistry* 51, no. 3 (2008): 677–683, https://doi.org/10.1021/jm7012776.

15. T. Vitha, V. Kubíček, J. Kotek, et al., "Gd (Iii) Complex of a Monophosphinate-Bis (Phosphonate) DOTA Analogue With a High Relaxivity; Lanthanide (Iii) Complexes for Imaging and Radiotherapy of Calcified Tissues," *Dalton Transactions* 17 (2009): 3204–3214, https://doi.org/10.1039/b820705d.

16. K. Suzuki, M. Satake, J. Suwada, et al., "Synthesis and Evaluation of a Novel 68Ga-Chelate-Conjugated Bisphosphonate as a Bone-Seeking Agent for PET Imaging," *Nuclear Medicine and Biology* 38, no. 7 (2011): 1011–1018, https://doi.org/10.1016/j.nucmedbio.2011.02.015.

17. M. Meckel, M. Fellner, N. Thieme, R. Bergmann, V. Kubicek, and F. Rösch, "In Vivo Comparison of DOTA Based 68Ga-Labelled Bisphosphonates for Bone Imaging in Non-Tumour Models," *Nuclear Medicine and Biology* 40, no. 6 (2013): 823–830, https://doi.org/10.1016/j.nucmedbio.2013.04.012.

18. Z. Wu, Z. Zha, S. R. Choi, K. Plössl, L. Zhu, and H. F. Kung, "New (68)Ga-PhenA Bisphosphonates as Potential Bone Imaging Agents," *Nuclear Medicine and Biology* 43, no. 6 (2016): 360–371, https://doi.org/10.1016/j.nucmedbio.2016.03.002.

19. A. Fakhari, A. R. Jalilian, F. Johari-Daha, M. Shafiee-Ardestani, and A. Khalaj, "Preparation and Biological Study of (68)Ga-DOTA-Alendronate," *Asia Oceania Journal of Nuclear Medicine and Biology* 4, no. 2 (2016): 98–105, https://doi.org/10.7508/aojnmb.2016.02.006.

20. M. Meckel, R. Bergmann, M. Miederer, and F. Roesch, "Bone Targeting Compounds for Radiotherapy and Imaging: *Me (III)-DOTA Conjugates of Bisphosphonic Acid, Pamidronic Acid and Zoledronic Acid," *EJNMMI Radiopharmacy and Chemistry* 1, no. 1 (2017): 14, https://doi.org/10.1186/s41181-016-0017-1.

21. M. Fellner, R. P. Baum, V. Kubícek, et al., "PET/CT Imaging of Osteoblastic Bone Metastases WITH (68)Ga-Bisphosphonates: First Human Study," *European Journal of Nuclear Medicine and Molecular Imaging* 37, no. 4 (2010): 834, https://doi.org/10.1007/s00259-009-1355-y.

22. R. Vatsa, D. Kaur, S. S. Shekhar, et al., "Comparison of 99mTc-Methylenediphosphonate and 68Ga-BPAMD PET/Computed Tomography Imaging in Bone Metastasis," *Nuclear Medicine Communications* 44 (2023): 463–470, https://doi.org/10.1097/MNM.0000000000001685.

23. R. Bergmann, M. Meckel, V. Kubíček, et al., "(177)Lu-Labelled Macrocyclic Bisphosphonates for Targeting Bone Metastasis in Cancer Treatment," *EJNMMI Research* 6, no. 1 (2016): 5, https://doi.org/10.1186/s13550-016-0161-3.

24. C. Bal, G. Arora, P. Kumar, et al., "Pharmacokinetic, Dosimetry and Toxicity Study of ^{177}Lu-EDTMP in Patients: Phase 0/I Study," *Current Radiopharmaceuticals* 9, no. 1 (2016): 71–84, https://doi.org/10.2174/1874471008666150313105000.

25. N. Salek, M. Mehrabi, S. Shirvani Arani, et al., "Production, Quality Control, and Determination of Human Absorbed Dose of no Carrier Added 177 Lu-Risedronate for Bone Pain Palliation Therapy," *Journal of Labelled Compounds and Radiopharmaceuticals* 60, no. 1 (2017): 20–29, https://doi.org/10.1002/jlcr.3466.

26. A. Khawar, E. Eppard, F. Roesch, et al., "Biodistribution and Post-Therapy Dosimetric Analysis of [177Lu]Lu-DOTAZOL in Patients With Osteoblastic Metastases: First Results," *EJNMMI Research* 9, no. 1 (2019): 102, https://doi.org/10.1186/s13550-019-0566-x.

27. Q. Wang, J. Yang, Y. Wang, et al., "Lutetium177-Labeled DOTA-Ibandronate: A Novel Radiopharmaceutical for Targeted Treatment of Bone Metastases," *Molecular Pharmaceutics* 20, no. 3 (2023): 1788–1795, https://doi.org/10.1021/acs.molpharmaceut.2c00978.

28. N. Pfannkuchen, N. Bausbacher, S. Pektor, M. Miederer, and F. Rosch, "In Vivo Evaluation of [225Ac]Ac-DOTAZOL for α-Therapy of Bone Metastases," *Current Radiopharmaceuticals* 11, no. 3 (2018): 223–230, https://doi.org/10.2174/1874471011666180604083911.

29. M. Fellner, R. Baum, V. Kubicek, P. Hermann, and F. Roesch, "177Lu-BPAMD—From Bone Imaging to Therapy With a Macrocycle-Bisphosphonate Ligand," *Journal of Nuclear Medicine* 51, no. supplement 2 (2010): 1164.

30. D. Mueller, I. Klette, and R. Baum, "Clinical Routine Production of 177Lu-BPAMD," *Journal of Nuclear Medicine* 54, no. supplement 2 (2013): 1191.

31. A. Rabiei, M. Shamsaei, H. Yousefnia, S. Zolghadri, A. R. Jalilian, and R. Enayati, "Development and Biological Evaluation of 90Y-BPAMD as a Novel Bone Seeking Therapeutic Agent," *Radiochimica Acta* 104, no. 10 (2016): 727–734, https://doi.org/10.1515/ract-2015-2561.

32. A. Rabiei, H. Yousefnia, S. Zolghadri, and M. Shamsaei, "Preliminary Dosimetric Evaluation of ^{90} Y-BPAMD as a Potential Agent for Bone Marrow Ablative Therapy," *Journal of Radiotherapy in Practice* 18, no. 1 (2019): 70–74, https://doi.org/10.1017/S146039691800047X.

33. A. Rabie, R. Enayati, H. Yousefnia, et al., "Preparation, Quality Control and Biodistribution Assessment of ^{153}Sm-BPAMD as a Novel Agent for Bone Pain Palliation Therapy," *Annals of Nuclear Medicine* 29, no. 10 (2015): 870–876, https://doi.org/10.1007/s12149-015-1014-2.

34. H. Yousefnia, N. Amraei, M. Hosntalab, S. Zolghadri, and A. Bahrami-Samani, "Preparation and Biological Evaluation of 166Ho-BPAMD as a Potential Therapeutic Bone-Seeking Agent," *Journal of Radioanalytical and Nuclear Chemistry* 304, no. 3 (2015): 1285–1291, https://doi.org/10.1007/s10967-014-3924-1.

35. S. Zolghadri and H. Yousefnia, "Human Organ Absorbed Dose Estimation of 166Ho-BPAMD Complex Based on Biodistribution Data of Male Syrian Rats," *Iranian Journal of Nuclear Medicine.* 27, no. 2 (2019): 87–91.

36. M. Vaez-Tehrani, S. Zolghadri, H. Afarideh, and H. Yousefnia, "Preparation and Biological Evaluation of 175Yb-BPAMD as a Potential Agent for Bone Pain Palliation Therapy," *Journal of Radioanalytical and Nuclear Chemistry* 309, no. 3 (2016): 1183–1190, https://doi.org/10.1007/s10967-016-4734-4.

37. M. Vaez-Tehrani, S. Zolghadri, H. Yousefnia, and H. Afarideh, "Human Absorbed Dose Estimation for a new (175)Yb-Phosphonate Based on Rats Data: Comparison with Similar Bone Pain Palliation Agents," *Applied Radiation and Isotopes* 115 (2016): 55–60, https://doi.org/10.1016/j.apradiso.2016.06.013.

38. C. Decristoforo, "Gallium-68 - A new Opportunity for PET Available From a Long Shelf-Life Generator—Automation and Applications," *Current Radiopharmaceuticals* 5, no. 3 (2012): 212–220, https://doi.org/10.2174/1874471011205030212.

39. C. Decristoforo, I. Penuelas, M. Patt, and S. Todde, "European Regulations for the Introduction of Novel Radiopharmaceuticals in the Clinical Setting," *Quarterly Journal of Nuclear Medicine and Molecular Imaging* 61, no. 2 (2017): 135–144, https://doi.org/10.23736/S1824-4785.17.02965-X.

40. J. Kleynhans, S. Rubow, J. le Roux, B. Marjanovic-Painter, J. R. Zeevaart, and T. Ebenhan, "Production of [^{68} Ga]Ga-PSMA: Comparing a Manual Kit-Based Method With a Module-Based Automated Synthesis Approach," *Journal of Labelled Compounds and Radiopharmaceuticals* 63 (2020): 553–563, https://doi.org/10.1002/jlcr.3879.

41. M. Fellner, B. Biesalski, N. Bausbacher, et al., "(68)Ga-BPAMD: PET-Imaging of Bone Metastases With a Generator Based Positron Emitter," *Nuclear Medicine and Biology* 39, no. 7 (2012): 993–999, https://doi.org/10.1016/j.nucmedbio.2012.04.007.

42. M. Guleria, T. Das, J. Amirdhanayagam, et al., "Convenient Formulation of 68Ga-BPAMD Patient Dose Using Lyophilized BPAMD Kit and 68Ga Sourced from Different Commercial Generators for Imaging of Skeletal Metastases," *Cancer Biotherapy & Radiopharmaceuticals* 34, no. 2 (2019): 67–75, https://doi.org/10.1089/cbr.2018.2605.

43. M. Meisenheimer, S. Kürpig, M. Essler, and E. Eppard, "DOTAZOL: A Promising Tool in Diagnosis and Palliative Therapy of Bone Metastasis-Challenges and Critical Points in Implementation Into Clinical Routine," *Molecules* 25, no. 13 (2020): 2988, https://doi.org/10.3390/molecules25132988.

44. C. Souche, J. Fouillet, L. Rubira, C. Donzé, E. Deshayes, and C. Fersing, "Bisphosphonates as Radiopharmaceuticals: Spotlight on the Development and Clinical Use of DOTAZOL in Diagnostics and Palliative Radionuclide Therapy," *IJMS.* 25, no. 1 (2023): 462, https://doi.org/10.3390/ijms25010462.

45. M. Bauwens, R. Chekol, H. Vanbilloen, G. Bormans, and A. Verbruggen, "Optimal Buffer Choice of the Radiosynthesis of 68Ga–Dotatoc for Clinical Application," *Nuclear Medicine Communications* 31, no. 8 (2010): 753–758, https://doi.org/10.1097/MNM.0b013e32833acb99.

46. A. Alfteimi, U. Lützen, A. Helm, et al., "Automated Synthesis of [68Ga]Ga-FAPI-46 Without Pre-Purification of the Generator Eluate on Three Common Synthesis Modules and Two Generator Types," *EJNMMI Radiopharmacy and Chemistry* 7, no. 1 (2022): 20, https://doi.org/10.1186/s41181-022-00172-1.

47. M. Meisenheimer, S. Kürpig, M. Essler, and E. Eppard, "Manual vs Automated ^{68} Ga-Radiolabelling-A Comparison of Optimized Processes," *Journal of Labelled Compounds and Radiopharmaceuticals* 63, no. 4 (2020): 162–173, https://doi.org/10.1002/jlcr.3821.

48. T. Daniel, C. Balouzet Ravinet, J. Clerc, R. Batista, and Y. Mouraeff, "Automated Synthesis and Quality Control of [68Ga]Ga-PentixaFor Using the Gaia/Luna Elysia-Raytest Module for CXCR4 PET Imaging," *EJNMMI Radiopharmacy and Chemistry* 8, no. 1 (2023): 4, https://doi.org/10.1186/s41181-023-00187-2.

49. A. Moyon, P. Garrigue, S. Fernandez, et al., "Comparison of a New 68Ga-Radiolabelled PET Imaging Agent sCD146 and RGD Peptide for In Vivo Evaluation of Angiogenesis in Mouse Model of Myocardial Infarction," *Cells* 10, no. 9 (2021): 2305, https://doi.org/10.3390/cells10092305.

50. B. Baur, C. Solbach, E. Andreolli, G. Winter, H. J. Machulla, and S. Reske, "Synthesis, Radiolabelling and In Vitro Characterization of the Gallium-68-, Yttrium-90- and Lutetium-177-Labelled PSMA Ligand, CHX-A"-DTPA-DUPA-Pep," *Pharmaceuticals.* 7, no. 5 (2014): 517–529, https://doi.org/10.3390/ph7050517.

51. E. de Blois, "Semi-Automated System for Concentrating 68Ga-Eluate to Obtain High Molar and Volume Concentration of 68Ga-Radiopharmaca for Preclinical Applications," *Nuclear Medicine and Biology* 64-65 (2018): 16–21.

52. M. W. Jornitz, "Integrity Testing," in *Sterile Filtration*. Advances in Biochemical Engineering, vol. 98, ed. M. W. Jornitz (Berlin/Heidelberg: Springer-Verlag, 2006): 143–180, https://doi.org/10.1007/b104248.

53. K. Eryilmaz, H. E. Bakar, and B. Kilbas, "Novel Developed HPLC Analyses of [68 Ga]Ga/[177 Lu]Lu-EDTMP and [68 Ga]Ga/[177 Lu]Lu-DOTA-Zoledronate," *Journal of Labelled Compounds and Radiopharmaceuticals* 65, no. 7 (2022): 178–186, https://doi.org/10.1002/jlcr.3972.

54. F. Pisaneschi and N. T. Viola, "Development and Validation of a PET/SPECT Radiopharmaceutical in Oncology," *Molecular Imaging and Biology* 24, no. 1 (2022): 1–7, https://doi.org/10.1007/s11307-021-01645-6.

55. B. J. B. Nelson, J. D. Andersson, F. Wuest, and S. Spreckelmeyer, "Good Practices for 68Ga Radiopharmaceutical Production," *EJNMMI Radiopharmacy and Chemistry* 7, no. 1 (2022): 27, https://doi.org/10.1186/s41181-022-00180-1.

56. I. Velikyan, U. Rosenstrom, and O. Eriksson, "Fully Automated GMP Production of [68Ga]Ga-DO3A-VS-Cys40-Exendin-4 for Clinical Use," *American Journal of Nuclear Medicine and Molecular Imaging* 7, no. 3 (2017): 111–125.

57. I. Velikyan, P. Schweighöfer, J. Feldwisch, J. Seemann, F. Y. Frejd, and J. Sörensen, "Diagnostic HER2-Binding Radiopharmaceutical, [68Ga]Ga-ABY-025, for Routine Clinical use in Breast Cancer Patients," *American Journal of Nuclear Medicine and Molecular Imaging* 9, no. 1 (2019): 12–23.

58. M. B. Haskali, "Automated Preparation of Clinical Grade [68Ga]Ga-DOTA-CP04, a Cholecystokinin-2 Receptor Agonist, Using iPHASE MultiSyn Synthesis Platform," *EJNMMI Radiopharmacy and Chemistry* 4 (2019): 23.

59. I. Velikyan, J. G. Doverfjord, S. Estrada, H. Steen, G. Van Scharrenburg, and G. Antoni, "GMP Production of [68Ga]Ga-BOT5035 for Imaging of Liver Fibrosis in Microdosing Phase 0 Study," *Nuclear Medicine and Biology* 88-89 (2020): 73–85.

60. J. Reverchon, F. Khayi, M. Roger, A. Moreau, and D. Kryza, "Optimization of the Radiosynthesis of [68Ga]Ga-PSMA-11 Using a Trasis MiniAiO Synthesizer: Do We Need to Heat and Purify?," *Nuclear Medicine Communications* 41, no. 9 (2020): 977–985, https://doi.org/10.1097/MNM.0000000000001233.

61. M. Wagner, J. G. Doverfjord, J. Tillner, et al., "Automated GMP-Compliant Production of [68Ga]Ga-DO3A-Tuna-2 for PET Microdosing Studies of the Glucagon Receptor in Humans," *Pharmaceuticals*. 13, no. 8 (2020): 176, https://doi.org/10.3390/ph13080176.

62. J. le Roux, S. Rubow, and T. Ebenhan, "A Comparison of Labelling Characteristics of Manual and Automated Synthesis Methods for Gallium-68 Labelled Ubiquicidin," *Applied Radiation and Isotopes* 168 (2021): 109452, https://doi.org/10.1016/j.apradiso.2020.109452.

63. M. Nader, K. Herrmann, F. Kunkel, et al., "Improved Production of 68Ga-Pentixafor Using Cartridge Mediated Cation Exchange Purification," *Applied Radiation and Isotopes* 189 (2022): 110447, https://doi.org/10.1016/j.apradiso.2022.110447.

64. K. Pohle, J. Notni, J. Bussemer, H. Kessler, M. Schwaiger, and A. J. Beer, "68Ga-NODAGA-RGD is a Suitable Substitute for 18F-Galacto-RGD and can be Produced With High Specific Activity in a cGMP/GRP Compliant Automated Process," *Nuclear Medicine and Biology* 39, no. 6 (2012): 777–784, https://doi.org/10.1016/j.nucmedbio.2012.02.006.

65. R. Martin, S. Jüttler, M. Müller, and H. J. Wester, "Cationic Eluate Pretreatment for Automated Synthesis of [68Ga]CPCR4.2," *Nuclear Medicine and Biology* 41, no. 1 (2014): 84–89, https://doi.org/10.1016/j.nucmedbio.2013.09.002.

66. A. Sammartano, S. Migliari, M. Scarlattei, G. Baldari, and L. Ruffini, "Synthesis, Validation and Quality Controls of [68Ga]-DOTA-Pentixafor for PET Imaging of Chemokine Receptor CXCR4 Expression: Synthesis and CQ of [68Ga]-DOTA-Pentixafor," *Acta Biomedica Atenei Parmensis*. 91, no. 4 (2020): e2020097, https://doi.org/10.23750/abm.v91i4.9106.

67. A. A. Hörmann, E. Plhak, M. Klingler, et al., "Automated Synthesis of 68Ga-Labeled DOTA-MGS8 and Preclinical Characterization of Cholecystokinin-2 Receptor Targeting," *Molecules* 27, no. 6 (2022): 2034, https://doi.org/10.3390/molecules27062034.

68. J. Greiser, T. Winkens, O. Perkas, C. Kuehnel, W. Weigand, and M. Freesmeyer, "Automated GMP Production and Preclinical Evaluation of [68Ga]Ga-TEoS-DAZA and [68Ga]Ga-TMoS-DAZA," *Pharmaceutics*. 14, no. 12 (2022): 2695, https://doi.org/10.3390/pharmaceutics14122695.

69. S. Migliari, M. Scarlattei, G. Baldari, and L. Ruffini, "Scale Down and Optimized Automated Production of [68Ga]68Ga-DOTA-ECL1i PET Tracer Targeting CCR2 Expression," *EJNMMI Radiopharmacy and Chemistry* 8, no. 1 (2023): 3, https://doi.org/10.1186/s41181-023-00188-1.

70. European Directorate for the Quality of Medicines & Healthcare (EDQM), "Gallium (68Ga) PSMA-11 Injection," *European Pharmacopoeia* 110, no. 3044 (2021): 1276–1277.

71. European Directorate for the Quality of Medicines & Healthcare (EDQM), "Gallium (68Ga) Edotreotide Injection," *European Pharmacopoeia* 110, no. 2482 (2022): 1274–1276.

72. G. J. Meyer, H. Mäcke, J. Schuhmacher, W. H. Knapp, and M. Hofmann, "68Ga-Labelled DOTA-Derivatised Peptide Ligands," *European Journal of Nuclear Medicine and Molecular Imaging* 31, no. 8 (2004): 1097–1104, https://doi.org/10.1007/s00259-004-1486-0.

73. R. Sasson, D. Vaknin, A. Bross, and E. Lavie, "Determination of HEPES in 68Ga-Labeled Peptide Solutions," *Journal of Radioanalytical and Nuclear Chemistry* 283, no. 3 (2010): 753–756, https://doi.org/10.1007/s10967-010-0449-0.

74. S. Pfaff, T. Nehring, V. Pichler, et al., "Development and Evaluation of a Rapid Analysis for HEPES Determination in 68Ga-Radiotracers," *EJNMMI Research* 8, no. 1 (2018): 95, https://doi.org/10.1186/s13550-018-0449-6.

75. I. F. Antunes, G. M. Franssen, R. Zijlma, P. Laverman, H. H. Boersma, and P. H. Elsinga, "New Sensitive Method for HEPES Quantification in 68Ga-Radiopharmaceuticals," *EJNMMI Radiopharmacy and Chemistry* 5, no. 1 (2020): 12, https://doi.org/10.1186/s41181-020-00093-x.

76. S. Migliari, M. Scarlattei, G. Baldari, C. Silva, and L. Ruffini, "A Specific HPLC Method to Determine Residual HEPES in [68Ga]Ga-Radiopharmaceuticals: Development and Validation," *Molecules* 27, no. 14 (2022): 4477, https://doi.org/10.3390/molecules27144477.

77. T. R. Theodore, R. L. Van Zandt, and R. H. Carpenter, "Pilot Ascending Dose Tolerance Study of Parenterally Administered 4-(2 Hydroxyethyl)-l-Piperazine Ethane Sulfonic Acid (TVZ-7) in Dogs," *Cancer Biotherapy & Radiopharmaceuticals* 12, no. 5 (1997): 345–349, https://doi.org/10.1089/cbr.1997.12.345.

78. T. R. Theodore, R. L. Van Zandt, and R. H. Carpenter, "Preliminary Evaluation of a Fixed Dose of Zwitterionic Piperazine (TVZ-7) in Clinical Cancer," *Cancer Biotherapy & Radiopharmaceuticals* 12, no. 5 (1997): 351–353, https://doi.org/10.1089/cbr.1997.12.351.

79. M. Guleria, K. J. Pallavi, P. P. Gujarathi, and T. Das, "Evaluation of Acute Intravenous Toxicity of HEPES: Is Good's Buffer Good and Safe Enough for Clinical Utilization in Nuclear Medicine?," *Nuclear Medicine and Biology* 132-133 (2024): 108895, https://doi.org/10.1016/j.nucmedbio.2024.108895.

80. J. le Roux, J. Kleynhans, and S. Rubow, "The use of HEPES-Buffer in the Production of Gallium-68 Radiopharmaceuticals – Time to Reconsider Strict Pharmacopoeial Limits?," *EJNMMI Radiopharmacy and Chemistry* 6, no. 1 (2021): 15, https://doi.org/10.1186/s41181-021-00129-w.

81. N. Lepareur, "Cold Kit Labeling: The Future of 68Ga Radiopharmaceuticals?," *Frontiers in Medicine* 9 (2022): 812050, https://doi.org/10.3389/fmed.2022.812050.

82. K. Ogawa, K. Takai, H. Kanbara, et al., "Preparation and Evaluation of a Radiogallium Complex-Conjugated Bisphosphonate as a Bone Scintigraphy Agent," *Nuclear Medicine and Biology* 38, no. 5 (2011): 631–636, https://doi.org/10.1016/j.nucmedbio.2010.12.004.

83. D. Zuccato and E. Guadagnino, "Glass for Pharmaceutical Use," in *Encyclopedia of Glass Science, Technology, History, and Culture* (Hoboken, NJ: John Wiley & Sons, Ltd, 2021): 879–889, https://doi.org/10.1002/9781118801017.ch7.7.

84. M. Meckel, V. Kubíček, P. Hermann, M. Miederer, and F. Rösch, "A DOTA Based Bisphosphonate With an Albumin Binding Moiety for Delayed Body Clearance for Bone Targeting," *Nuclear Medicine and*

Biology 43, no. 11 (2016): 670–678, https://doi.org/10.1016/j.nucmedbio.2016.07.009.

85. S. F. Garcia-Arguello, B. Lopez-Lorenzo, and R. Ruiz-Cruces, "Automated Production of [68Ga]Ga-DOTANOC and [68Ga]Ga-PSMA-11 Using a TRACERlab FXFN Synthesis Module," *Journal of Labelled Compounds and Radiopharmaceuticals* 62, no. 3 (2019): 146–153.

86. S. Spreckelmeyer, M. Balzer, S. Poetzsch, and W. Brenner, "Fully-Automated Production of [68Ga]Ga-FAPI-46 for Clinical Application," *EJNMMI Radiopharmacy and Chemistry* 5, no. 1 (2020): 31, https://doi.org/10.1186/s41181-020-00112-x.

87. C. Da Pieve, M. Costa Braga, D. R. Turton, et al., "New Fully Automated Preparation of High Apparent Molar Activity 68Ga-FAPI-46 on a Trasis AiO Platform," *Molecules* 27, no. 3 (2022): 675, https://doi.org/10.3390/molecules27030675.

Supporting Information

Additional supporting information can be found online in the Supporting Information section.